Effects of the Surface Roughness on the Dynamics of a Rotor Supported by Aerostatic Bearing

Abdurrahim Dal and Tuncay Karaçay

***Abstract*—In this study, effects of surface roughness of the bearing surface on the dynamic of a rotor supported by aerostatic bearing are theoretically investigated. In order to analyze the dynamics of the bearing-rotor system, air flow between rotor and bearing surfaces is modelled using the Reynold's equation. In this air flow model, clearance function which is given geometrical relation between rotor and bearing surface, is defined with surface roughness. Then, the air film model is solved by Differential Transform & Finite Difference hybrid numerical solution method to obtain air film forces. In order to investigate the effect of the surface roughness on the dynamic motions of the bearing-rotor system, the system is modelled in two degrees-of-freedom with the air film forces, and this model is simulated for different values of surface roughness and different rotor mass.**

***Index Terms*—Air bearing, clearance function, load carrying capacity, surface roughness**

I. Introduction

In the aerostatic bearing, air separates rotor and bearing surfaces and generates a thin film between these surfaces. This film gives advantages to the bearing-rotor system such as low friction resistance and long component life due to its low viscosity. So, the externally pressurized air lubricated (aerostatic) bearing-rotor systems should be suitable for high precision and high speed applications [1].

The dynamics of the rotor-bearing system supported by aerostatic bearing is directly related to air film forces. In the aerostatic bearing, this air film forces are generated by pressure distribution, in other words air flow between rotor and bearing surfaces, and the air flow is affected by geometrical parameters of the aerostatic bearing such as radial clearance, L/D ratio, supply holes location on the bearing and geometrical properties of supply holes [2]. In addition, roughness of the aerostatic bearing and/or the rotor surfaces changes the gap between them and it also influences the air flow between the rotor and the bearing surfaces. So, the surface roughness is also affected the dynamic of the rotor-bearing system, besides other geometrical parameters of aerostatic bearing. In the literature, effects of geometrical parameters on the dynamics of a rotor supported by aerostatic bearing are investigated in detail. Larson and Richardson [3] presented experimental data for threshold of whirl instability for a rigid rotor supported by externally pressurized gas bearing with different supply pressure and different radial clearance. Majumdar [4] analyzed flow and load characteristic of an externally pressurized gas journal bearing in his theoretically study. He presented these flow and load expressed in dimensionless factors for different bearing design parameters such as radial clearance, L/D ratio and configuration of feeding system. Cunningham *et al.* [5] theoretically and experimentally analyzed critical speed of a rotor supported by externally pressurized air bearings. In their theoretical investigation, the air bearing-rotor system was modelled taking into account the rocking motion of the rotor. Besides, in their test rig, a rotor supported by externally pressurized air bearings is located in a vertical position and they measured radial motion of rotor for different radial clearances and different supply pressures. Stouth [6] theoretically analyzed effect of manufacturing variations on the performance of externally pressurized gas journal bearing. He investigated effects of bearing clearance, feed slot thickness, bearing form, bearing roundness, bearing member alignment and feed slot geometry on the load carrying capacity of the bearing and he gave design parameters for externally pressurized air journal bearing with slot restrictors. Han *et al* [7] theoretically and experimentally investigated the dynamics characteristic of a rotor supported in the externally pressurized air bearing for different geometric parameters and different operational conditions such as L/D ratio, number of supply holes, supply holes diameter, supply pressure, rotor angular speeds. Lo *et al.* [8] discretized Reynold's equation by use Newton method and investigated load carrying capacity and stiffness for different supply pressure, L/D ratio and radial clearance. Chen *et al*. [9] investigated stiffness of various geometric designs of aerostatic journal bearings for high-speed spindles under different operating conditions. They evaluated the stiffness experimentally using the relationship of force and displacement at different supply pressures. They concluded that the stiffness could be improved with high supply pressure, high L/D ratio and increased orifice diameter. Zhang *et al.* [10] derived the Reynold's equation with slip effect and they analyzed effects of bearing length-diameter ratio and slip on the stability and performance of gas journal bearing in micro electro mechanical systems.

Manuscript received March 17, 2016. This work was supported in part by the Scientific and Research Council of Turkey under Grant 112M847.

A. Dal is with the Gazi University, Engineering Faculty, Mechanical Engineering Department, Maltepe, 06570, Ankara, Turkey (phone: +90-312-582-3464; fax: +90-312-230-8434; e-mail: abdurrahimdal@gazi.edu.tr).

T. Karaçay is with the Gazi University, Engineering Faculty, Mechanical Engineering Department, Maltepe, 06570, Ankara, Turkey (e-mail: karacay@gazi.edu.tr).

ISBN: 978-988-14048-0-0
ISSN: 2078-0958 (Print); ISSN: 2078-0966 (Online)

White *et al.* [11-12] numerically investigated the effects of sinusoidal transverse roughness pattern in wedge air bearing on the characteristic of the ultra thin gas film. Raad and Kuria [13] researched the effects of two-sided surface roughness amplitude on ultra-thin, compressible, isothermal, infinitely wide gas bearings. Their results showed that introducing roughness on either bearing surface causes an increase in the load carrying capacity as compared to the smooth bearing case, when roughness is introduced on the stationary surface, the gas bearing generates higher loads and the load peaks increase quadratically with increasing stationary roughness amplitude. In addition, they concluded that the load becomes dependent on the amplitude of the surface roughness and not its location.

In literature, many studies on the effect of bearing design parameters such as radial clearance, L/D ratio on the dynamic and the performance of the bearing-rotor system were analyzed [3-10], In these studies, the surface of the bearing and/or the rotor are assumed to be smooth, in order words, effect of the surface roughness on the dynamic of the system was neglected. However, surface roughness effect was only analyzed for slider air bearing application such as hard disk drives [11-15].

In this study, effects of surface roughness on the dynamics of a rotor supported by aerostatic journal bearing are theoretically investigated. Firstly, air flow between rotor and bearing surfaces is modelled using Reynold's equation. In this air flow model, clearance function which is given geometrical relation of the rotor and the bearing surface, is defined with the surface roughness. Then, the air film model is solved by Differential Transform & Finite Difference (DTM&FDM) hybrid numerical solution method to obtain air film forces. In order to investigate the effect of the surface roughness on the dynamic motions of the bearing-rotor system, equations of motion of the system are obtained using Newton's second law of motion in two degrees-of-freedom with the air film forces and this model is simulated for different values of surface roughness and different rotor mass.

II. MATHEMATICAL MODEL

In the aerostatic bearings, thin air film separates the rotor and bearing surfaces and it supports the rotor. So, air film directly affects dynamics of the rotor supported the aerostatic bearing. In this section, mathematical model of air film and equations of motion of the rotor-bearing system are given.

A. Mathematical Model of Air Film

The configuration of aerostatic bearing-rotor system, orifices layout and coordinate system are given in Fig. 1. In the aerostatic bearings, air flow between the rotor and bearing surfaces is modelled using Reynold's equation for compressible flow, and it is given in (1). In the Reynold's equation, it assumed that flow is isothermal process, inertia effect is neglect and viscosity is constant due to geometrical structure of aerostatic journal bearing-rotor system and thermodynamic properties of air.

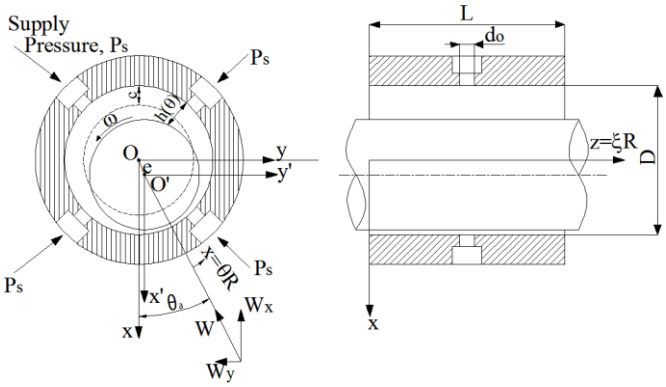

Fig. 1. Configuration of aerostatic bearing-rotor system

$$\frac{\partial}{\partial x}\left[\frac{h^3 p}{\mu}\frac{\partial p}{\partial x}\right]+\frac{\partial}{\partial z}\left[\frac{h^3 p}{\mu}\frac{\partial p}{\partial z}\right]+12R^0T^0\dot{m}=12\frac{\partial}{\partial t}(ph) +6U\frac{\partial}{\partial x}(ph) \tag{1}$$

where μ is viscosity, p is pressure, x and z are coordinate axis, $\dot{m}$ is mass flow rate and h is clearance function and it is defined as (2) with surface roughness.

$$h(\theta,\xi)=h_0(\theta,\xi)+h_r(\theta,\xi) \tag{2}$$

where h_0 represents smooth bearing surface and it is defined as (3), h_r is surface roughness part of the clearance function In this study, surface roughness part of the clearance function (see (2)) consists of random numbers which are generate in Matlab environment with Gaussian distribution.

$$h_0(\theta,\xi)=c+e\cos(\theta-\theta_a) \tag{3}$$

where c is the clearance between rotor and bearing surface, θ and ξ are circumferential and axial coordinate axis respectively, and θ_a represents attitude angle.

Reynold's equation could be given as (4) with dimensionless parameters which are given below;

$$P=pP_a,\ H=h/c,\ \theta=x/R,\ \xi=z/R,$$

$$U=r\omega,\ \sigma=\frac{12\mu}{P_a}\left(\frac{R}{c}\right)^2,\ \Lambda=\frac{6\mu\omega}{P_a}\left(\frac{R}{c}\right)^2$$

$$-\frac{\partial}{\partial\theta}\left[H^3P\frac{\partial P}{\partial\theta}\right]-\frac{\partial}{\partial\xi}\left[H^3P\frac{\partial P}{\partial\xi}\right]+\Lambda\frac{\partial}{\partial\theta}(PH) +\sigma\frac{\partial}{\partial t}(PH)=\dot{M} \tag{4}$$

where H is dimensionless clearance function, P is dimensionless pressure and $\dot{M}$ represents mass flow rate (see Ref. [16] for detail).

B. Equations of Motion of the Rotor-Bearing System

In this study, radial motion of the rotor supported by an aerostatic bearing is modelled in two degrees-of-freedom. The equations of motion of the bearing-rotor system, based

ISBN: 978-988-14048-0-0
ISSN: 2078-0958 (Print); ISSN: 2078-0966 (Online)

on the Newton's second law of motion and considering the Jeffcott rotor model, could be given as (5).

$$\begin{aligned} m\ddot{x} + W_x &= 0 \\ m\ddot{y} + W_y &= 0 \end{aligned} \tag{5}$$

In these equations of motion, there are no external forces applied the rotor and it is assumed that the rotor is balanced.

III. NUMERICAL SOLUTION TECHNIQUE

In the aerostatic bearing-rotor systems, air film forces directly affect dynamics of the rotor. In order to investigate dynamic motions of the rotor, firstly, the air film forces must be obtained by solving Reynold's equation and then, equation of motions must be solved with these air film forces.

A. Solution of Reynold's Equation

Reynold's equation which is given in (4), could be solved numerically to obtain pressure distribution between rotor and bearing surfaces. In this study, the Reynold's equation is solved using the DTM&FDM hybrid numerical method. The Differential Transform method is based on Taylor series expansion and widely used for solving differential equation due to minimum calculation error and rapid convergence [17]. In order for the numerical integration of the Reynold's equation, the DTM&FDM hybrid numerical solution method could be applied on a *MxN* uniform grid with the circumferential and axial coordinates as schematically illustrated in Fig. 2.

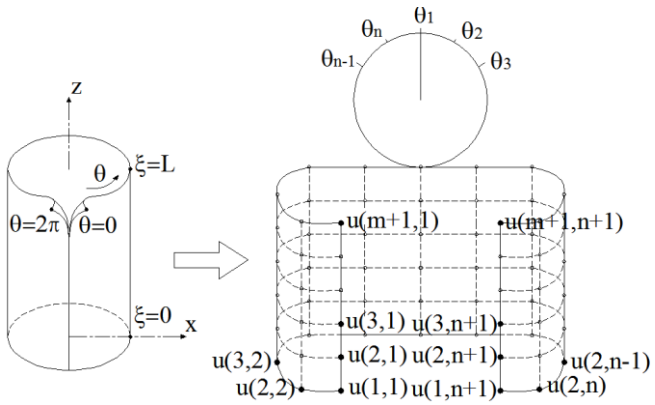

Fig. 2. Numerical solution grid

In order to apply the DTM&FDM hybrid numerical solution method, Reynold's equation could be linearized as (6).

$$\begin{aligned} &-3H^2\left(\frac{\partial H}{\partial\theta}\frac{\partial\Theta}{\partial\theta}+\frac{\partial H}{\partial\xi}\frac{\partial\Theta}{\partial\xi}\right)-H^3\left(\frac{\partial^2\Theta}{\partial\theta^2}+\frac{\partial^2\Theta}{\partial\xi^2}\right) \\ &+\Lambda\frac{H}{P}\frac{\partial\Theta}{\partial\theta}+2\Lambda P\frac{\partial H}{\partial\theta}+\sigma\frac{H}{P}\frac{\partial\Theta}{\partial t}+2\sigma P\frac{\partial H}{\partial t}=2\dot{M} \end{aligned} \tag{6}$$

where Θ is equal to P^2. The terms of in (6) could be transformed by using the Differential Transform theory, with respect to time domain, and hence (6) becomes,

$$\begin{aligned} &-3\mathrm{I}\otimes\frac{dH}{d\theta}\otimes\frac{d\Theta}{d\theta}-J\otimes\frac{d\Theta}{d\theta}-3I\otimes\frac{dH}{d\xi}-J\otimes\frac{d\Theta}{d\xi} \\ &+2\Lambda\otimes\frac{dH}{d\theta}\otimes P+2\Lambda\otimes\frac{dP}{d\theta}\otimes H+4\Lambda\otimes\frac{dH}{d\tau}\otimes P \\ &+4\Lambda\otimes\frac{dP}{d\tau}\otimes H=2\dot{M} \end{aligned} \tag{7}$$

where $\otimes$ is signified convolution operators in *K* domain and, in (7), using Differential Transform theory, I, J and Θ could be written as (8), (9) and (10) respectively.

$$I(k)=H\otimes H=\sum H\,(k-l)H\,(l) \tag{8}$$

$$J(k)=H\otimes H\otimes H=\sum H\,(k-l)\sum H\,(l-m)H\,(m) \tag{9}$$

$$\Theta(k)=P\otimes P=\sum P(k-l)P(l) \tag{10}$$

The Finite Difference method could be used to discretized the transformed Reynold's equation which is given in (7). Substituting (8)-(10) into (7), and it can be discretized using the second order central finite difference scheme. First term of the Reynold's equation could be written as in (11) and other terms could also be discretized correlatively (similar to the expansion in [17]).

$$\begin{aligned} &-3\mathrm{I}\otimes\frac{dH}{d\theta}\otimes\frac{d\Theta}{d\theta}= \\ &-3\sum_{l=0}^{k}\mathrm{I}_{i,j}(k-l)\sum_{m=0}^{l}\left(\left[\frac{H_{i,j+1}(l-m)-H_{i,j-1}(l-m)}{2\Delta\theta}\right]\right. \\ &\left.\left[\frac{\Theta_{i,j+1}(m)-\Theta_{i,j-1}(m)}{2\Delta\theta}\right]\right) \end{aligned} \tag{11}$$

In (11), *i* and *j* indicate the node position on the *MxN* grid at ξ and θ coordinate axes, respectively, and *k*, *l* and *m* indicate *k*th, *l*th and *m*th terms of transformation, respectively. $P_{i,j}(k)$, which represents the pressure distribution, could be calculated for each time interval from (11). In this study, in order to guaranteed the develop of fluid (air) flow within the radial clearance, a convergence criteria (C_{cr}) is defined in the routine of solution method as (12).

$$\frac{P_{i,j}^{\,n+1}-P_{i,j}^{\,n}}{P_{i,j}^{\,n+1}}<10^{-6} \tag{12}$$

In the solution of the Reynold's equation, initial pressure value of the nodes on the grid is set to atmospheric pressure, and then following boundary conditions are assumed;

1) Pressure values are equal to atmospheric pressure on the both ends of the bearing, $P(0,\theta)= P(L,\theta)=P_a$
2) Pressure distribution is a periodic function;
$$P(\xi,\theta)=P(\xi,\theta+2\pi),\ \left.\frac{\partial P}{\partial\theta}\right|_{\theta}=\left.\frac{\partial P}{\partial\theta}\right|_{\theta+2\pi}$$
3) Pressure distribution is symmetric to the centre of bearing length.

B. Dynamic Motions of the Bearing-Rotor System

Equation of motions of the bearing-rotor system are already given in (5). Dynamic motions of the rotor-bearing

ISBN: 978-988-14048-0-0
ISSN: 2078-0958 (Print); ISSN: 2078-0966 (Online)

system directly relate to the air flow in the radial clearance. So, an iterative procedure must be used to obtain dynamic motions of the rotor. In this study, an algorithm are developed in Matlab for obtain dynamic motions of the system. Flow chart of this algorithm is illustrated in Fig. 3.

The algorithm is started with geometric properties of air bearing and initial conditions. Then pressure distribution in clearance is obtained by solving Reynold's equation with DTM&FDM hybrid numerical solution method and air film forces are calculated by integrating pressure distribution over the rotor circumference and length direction; force distribution could be estimated as (13). Next, the value of acceleration, velocity and displacement of the rotor is estimated forth order Runge-Kutta method. Finally, these value of displacement and velocity, pressure distribution and component force to be new initial conditions for second time step and the algorithm will repeat to step-by-step until simulation time is finished.

$$W_x = p_a R^2 \int_0^{2\pi} \int_0^{L/R} P(\xi,\theta)\cos\theta d\xi d\theta$$
$$W_y = p_a R^2 \int_0^{2\pi} \int_0^{L/R} P(\xi,\theta)\sin\theta d\xi d\theta \quad (13)$$

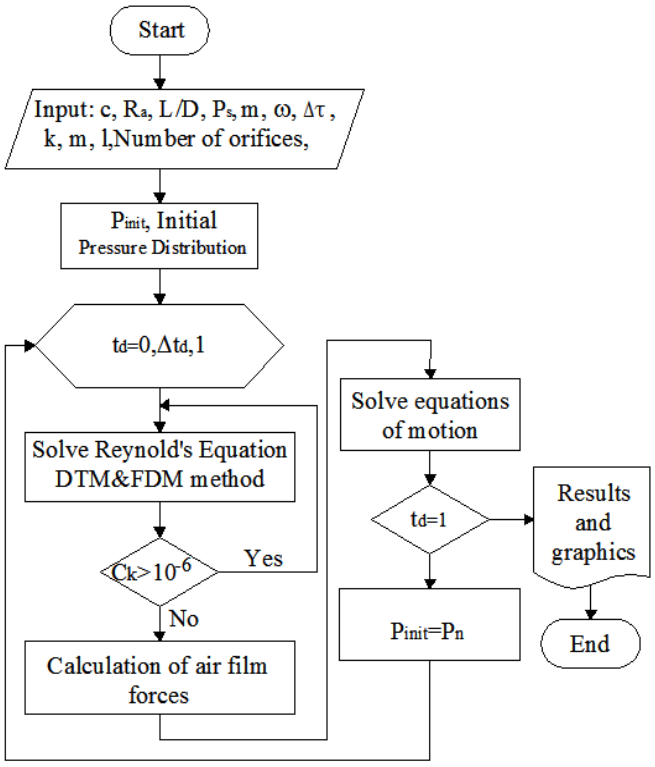

Fig. 3. Flow chart of solution algorithm

IV. RESULTS AND DISCUSSIONS

In this study, dynamics of the rotor supported by aerostatic bearing are investigated for different surface roughness of aerostatic bearing. In the simulation, it is assumed that the bearing surface is rough, as the rotor surface is smooth. The aerostatic bearing using in the simulation has four supply holes (see Fig. (1)), geometrical properties of the aerostatic bearing and thermodynamics properties of air are given in Table 1.

TABLE I
BEARING DETAİL

Symbol	Quantity	Value
c	radial clearance	$75x10^{-6}$ m
L	bearing length	0.05 m
D	bearing diameter	0.025 m
L/D	bearing length-diameter ration	2
d_o	supply hole diameter	$3x10^{-3}$ m
P_s	supply pressure	3 atm
μ	viscosity	$17.4x10^{-6}$
R^0	gas constant	287.6 J/Kg.K
T^0	absolute Temperature	288 °K
ω	angular speed of the rotor	1000 rad/s
-	number of orifices	4

A. The Bearing Surfaces

In order to investigate effect of surface roughness on the dynamics of the rotor-bearing system, several rough surfaces with various mean values, shown in Table 2, are generated in Matlab environment and a sample of the rough surface is given in Fig. 4. All generated surfaces are randomly distributed with Gaussian distribution.

TABLE 2
STATISTICAL PARAMETERS OF MODELED SURFACES

Surface	Mean (R_a)	Skewness	Kurtosis
1	5 μm	0	3
2	10 μm	0	3
3	15 μm	0	3

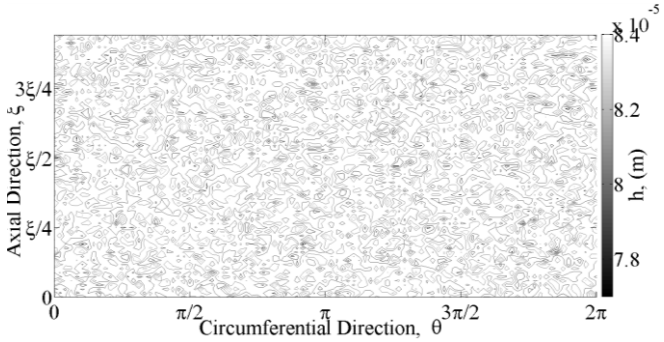

Fig. 4. A sample generated surface R_a=5 μm

B. Load Carrying Capacity

Load carrying capacity is the sum of forces produced by air film in radial clearance (see Eq. (13)). So, the load carrying capacity is affected by parameters of the surface roughness. Fig. 5 shows the variation of the load carrying capacity with respect to the eccentricity ratio for different surface types. Although the load carrying capacity is increased with eccentricity ratio values from *0* to *0.5* for all cases. The load performance of aerostatic bearing is decreased with higher values than *ε=0.5,* because pressurized air loose the compressibility characteristic in more smaller radial clearance. The relation between the load carrying capacity and the surface roughness is nearly same for eccentricity values from *ε=0* to *ε=0.5,* nevertheless the

ISBN: 978-988-14048-0-0
ISSN: 2078-0958 (Print); ISSN: 2078-0966 (Online)

value of load carrying capacity of smooth surface is a little bit higher at these eccentricity range. On the other hand, the load carrying capacity is higher for higher value of the surface roughness, when the eccentricity ratio is higher than *0.5*.

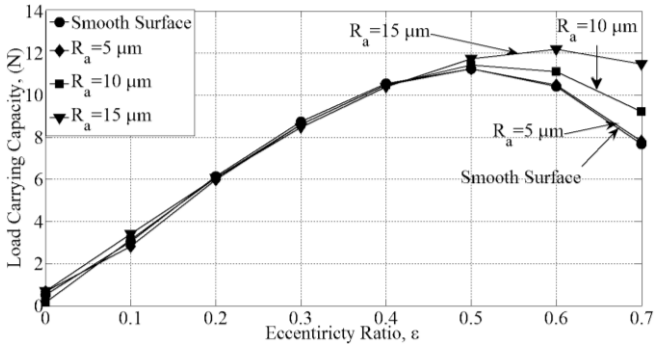

Fig. 5. Variations of load carrying capacity with respect to eccentricity ratio

C. *Dynamic Motions of the Bearing-Rotor System*

. In order to investigate the effects of the surface roughness on the dynamics motions of a rotor system supported by aerostatic bearings, a series of simulation runs are undertaken for the rotor-bearing configuration which is given in Table 1, and mass of rotor is equal to *0.5 kg* in simulations. Fig. 6 to Fig. 9 show vibration of the rotor at x-direction for different surface roughness and smooth surface. Amplitude of the vibration is decreased for higher value of surface roughness. Because the rotor-bearing system has higher value of load carrying capacity with increasing surface roughness (see Fig. 5). Besides, the steady state point at x-direction is getting closer to the center of the aerostatic bearing.

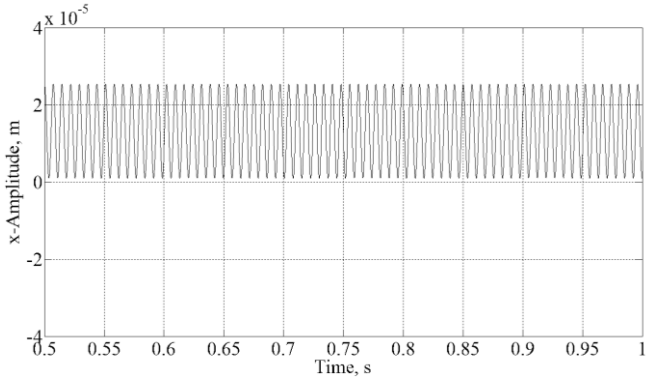

Fig. 6. Vibration of the rotor at x-direction for smooth surface

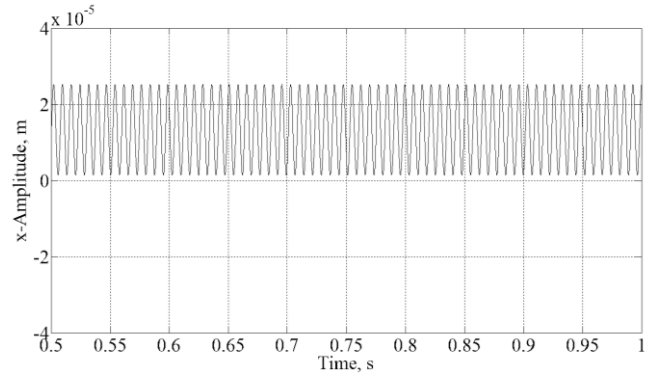

Fig. 7. Vibration of the rotor at x-direction for R_a=5 μm

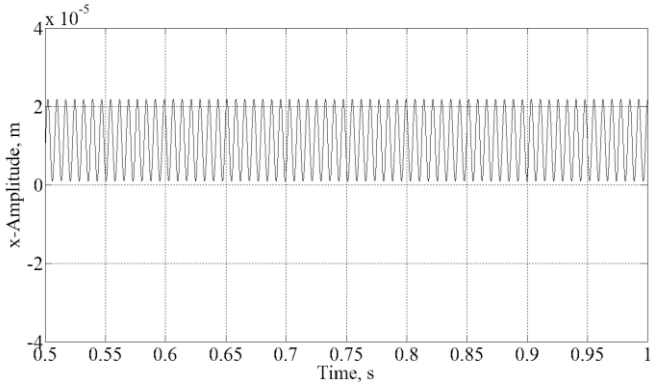

Fig. 8. Vibration of the rotor at x-direction for R_a=10 μm

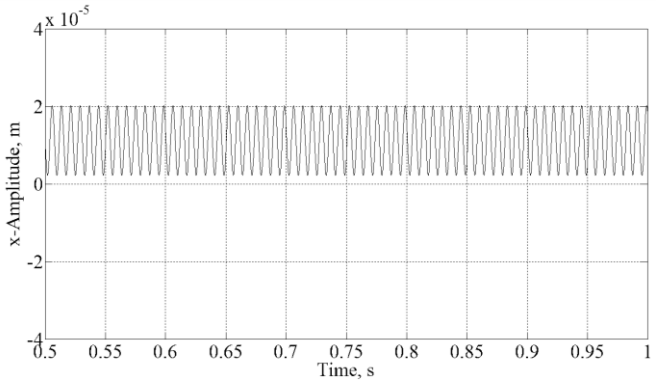

Fig. 9. Vibration of the rotor at x-direction for R_a=15 μm

Fig. 10 and Fig 11 show orbital behaviour of the rotor-bearing system for different surface roughness. In the orbit diagrams, effect of the surface roughness on the vibration of the system is also clearly seen. The orbit curve of the rotor center becomes narrow with increasing surface roughness

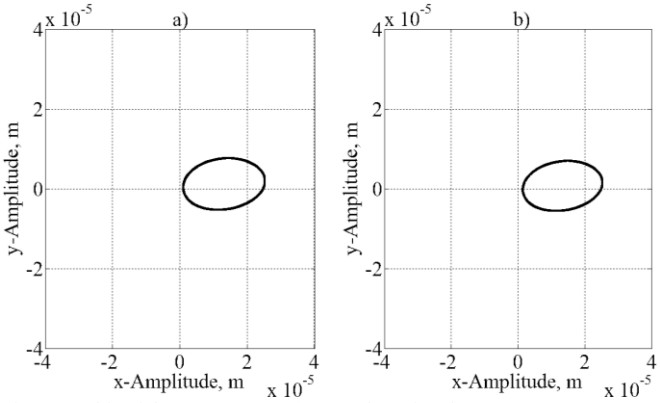

Fig. 10. Orbit of the rotor center, a) Smooth surface b) R_a=5 μm

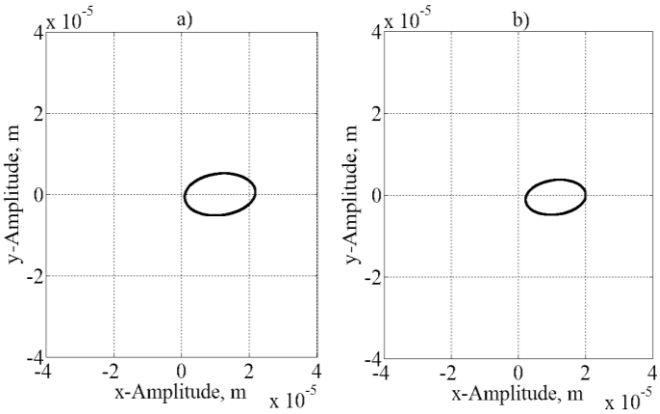

Fig. 11. Orbit of the rotor center a) R_a=10 μm b) R_a=15 μm

ISBN: 978-988-14048-0-0
ISSN: 2078-0958 (Print); ISSN: 2078-0966 (Online)

In order to investigate the effect of the surface roughness on the dynamic of the bearing-rotor system with rough bearing surface, a series simulation are also undertaken. The variations of the eccentricity of the rotor center with respect to the surface roughness are shown in Fig. 12. The eccentricity is increased with the increase of rotor mass, in other words the rotor oscillates at the point which has a distance to the center of the bearing, as expected. However, the eccentricity is decreased with increasing the surface roughness. Because the load carrying capacity is increased with the increase of the surface roughness for especially higher eccentricities.

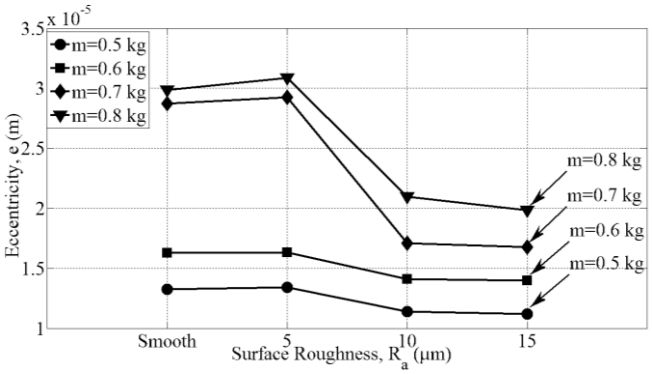

Fig. 12. Variations of the eccentricity of the rotor center with respect to surface roughness for different rotor mass

V. Conclusion

In this paper, effects of surface roughness on the dynamics of a rotor supported by aerostatic journal bearing are theoretically investigated. Firstly, air flow between rotor and bearing surfaces is modelled using Reynold's equation. In this air flow model, clearance function which is given geometrical relation of the rotor and the bearing surface, is defined with the surface roughness. Then, the air film model is solved by DTM&FDM hybrid solution method and, the equations of motion of the system in two degrees-of-freedom are simulated. Results show that the load carrying capacity is increased with higher value of surface roughness for higher eccentricity of the rotor center. So, the amplitude of vibration of the rotor-bearing system is lower for higher value surface roughness. Besides, the weighty rotor oscillates at the point which is closer the bearing center for higher surface roughness.

References

[1] N. Powell and J. Powell, *Gas Lubricated Bearings*, Butterworths Publishing, London, UK, (1964).
[2] J. Powell, *Design of aerostatic bearings*, Machinery's Books for Engineers, Machinery Publishing Co. Ltd. UK, (1970)
[3] R. H. Larson and H. H. Richardson, "A Preliminary Study Of Whirl Instability For Pressurized Gas Bearings," *ASME Journal of Basic Engineering.,* vol. 84, no 4, 1962 pp. 511-518.
[4] B. C. Majumdar, "Analysis of externally pressurized gas journal bearing", *Journal of Mechanical Science,* vol. 12, no 1, Feb. 1970, pp. 1-8.
[5] R. Cunningham, E. Gunter and L. R. Center, "Critical Speeds of a Rotor in Rigidly Mounted, Externally Pressurized Air-lubricated Bearings," NASA, Technical Report, NASA-TN-D-6350, E-6134, 1971.
[6] K. J. Stouth, "The effect of manufacturing variations on the performance of externally pressurized gas-lubricated journal bearings," *Proc. of the Ins. of Mech. Eng. Part C: Journal of Mechanical Engineering Science,* vol. 199, no. 4, 1985 pp. 299-309.
[7] D. Han, S. Park, W. Kim and J. Kim, "A study on the characteristics of externally pressurized air bearings," *Precision Engineering,* vol. 16, no 3, 1994 pp. 164-173.
[8] C. Lo, C. Wang and Y. Lee, "Performance Analysis Of High-Speed Spindle Aerostatic Bearings," *Tribology International*, vol. 38, 2005 pp. 5–14.
[9] Y. Chen, C. Chiu and Y. Cheng, "Influences of operational conditions and geometric parameters on the stiffness of aerostatic journal bearings," *Precision Engineering*, vol. 34, no 4, 2010 pp. 722-734.
[10] W-M. Zhang, J-B. Zhou and G. Meng, "Performance and stability analysis of gas-lubricated journal bearings in MEMS," *Tribology International* vol. 44, 2011 pp. 887-897
[11] J. W. White, P. E. Tabrizi, A. H. Ketkar and P. P. Prabbu, "A numerical study of surface roughness on ultra-thin gas films," *ASME J. Tribol.,* vol. 108, 1986 pp. 171-177.
[12] J. W. White and P. E. Raad, "Effect of a rough translating surface on gas film lubrication," *ASME J. Tribol.,* vol. 109, 1987 pp. 271-275.
[13] P. E. Raad and I. M. Kuria, "Two side texture effects on ultra-thin wide wedge gas bearings," *ASME J. Tribol.,* vol. 111, 1989 pp. 719-725.
[14] J. W. White, "The effect of two-dimensional surface roughness on the load carrying capacity of a thin compressible gas film," *ASME J. Tribol.,* vol. 115, 1993 pp.246-252.
[15] J. W. White, "Surface roughness effects on air bearing performance over a wide range of Kdunsen and Wave numbers," *ASME J. Tribol.,* vol. 132, 2010 pp.031703-1-10.
[16] A. Dal and T. Karaçay, "On dynamics of an externally pressurized air bearing with high values of clearance: Effect of mass flow rate," in *Lecture Notes in Engineering and Computer Science: World Congress on Engineering 2014,* pp. 1350–1355.
[17] C-C Wang and H-T Yau, "Theoretical analysis of high speed spindle air bearings by a hybrid numerical method," *Applied Mathematics and Computation*, 217 (5) (2010) 2084-2096.

ISBN: 978-988-14048-0-0
ISSN: 2078-0958 (Print); ISSN: 2078-0966 (Online)